Cell Reports, Volume *29*

Supplemental Information

Mass Cytometry Reveals Global Immune Remodeling with Multi-lineage Hypersensitivity to Type I Interferon in Down Syndrome

Katherine A. Waugh, Paula Araya, Ahwan Pandey, Kimberly R. Jordan, Keith P. Smith, Ross E. Granrath, Santosh Khanal, Eric T. Butcher, Belinda Enriquez Estrada, Angela L. Rachubinski, Jennifer A. McWilliams, Ross Minter, Tiana Dimasi, Kelley L. Colvin, Dmitry Baturin, Andrew T. Pham, Matthew D. Galbraith, Kyle W. Bartsch, Michael E. Yeager, Christopher C. Porter, Kelly D. Sullivan, Elena W. Hsieh, and Joaquin M. Espinosa

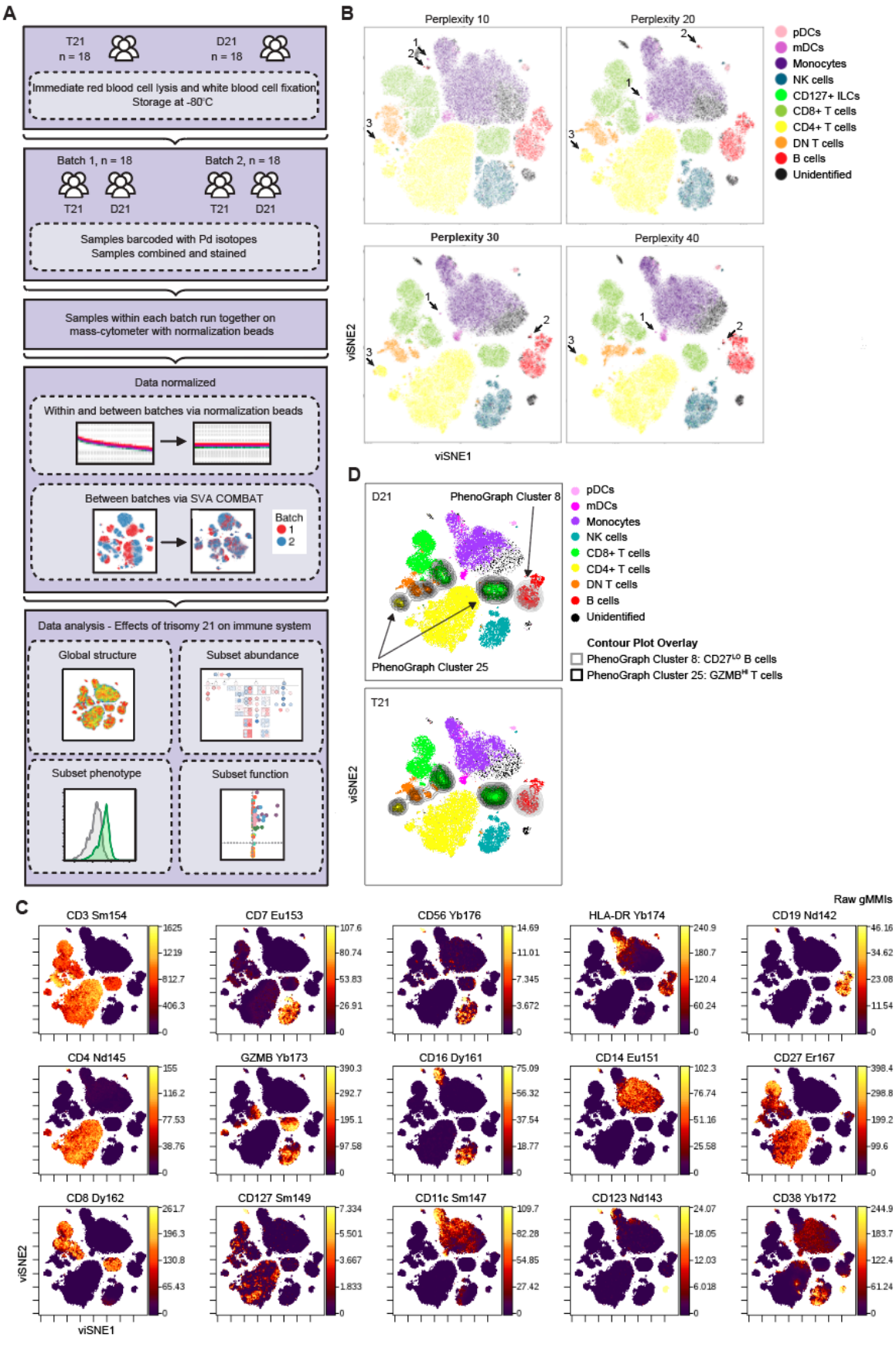
A
T21
n = 18
D21
n = 18
Immediate red blood cell lysis and white blood cell fixation
Storage at -80°C
Batch 1, n = 18
Batch 2, n = 18
T21
D21
T21
D21
Samples barcoded with Pd isotopes
Samples combined and stained
Samples within each batch run together on mass-cytometer with normalization beads
Data normalized
Within and between batches via normalization beads
Between batches via SVA COMBAT
Batch
1
2
Data analysis - Effects of trisomy 21 on immune system
Global structure
Subset abundance
Subset phenotype
Subset function
B
Perplexity 10
Perplexity 20
Perplexity 30
Perplexity 40
viSNE2
viSNE1
pDCs
mDCs
Monocytes
NK cells
CD127+ ILCs
CD8+ T cells
CD4+ T cells
DN T cells
B cells
Unidentified
D
D21
PhenoGraph Cluster 8
PhenoGraph Cluster 25
T21
viSNE2
pDCs
mDCs
Monocytes
NK cells
CD8+ T cells
CD4+ T cells
DN T cells
B cells
Unidentified
Contour Plot Overlay
PhenoGraph Cluster 8: CD27LO B cells
PhenoGraph Cluster 25: GZMBHI T cells
C
Raw gMMIs
CD3 Sm154
CD7 Eu153
CD56 Yb176
HLA-DR Yb174
CD19 Nd142
CD4 Nd145
GZMB Yb173
CD16 Dy161
CD14 Eu151
CD27 Er167
CD8 Dy162
CD127 Sm149
CD11c Sm147
CD123 Nd143
CD38 Yb172
viSNE2
viSNE1

Figure S1, related to Figure 1. **Mass cytometry analysis to characterize the immune system of adults with trisomy 21. (A)** Overview of the analysis pipeline used to define changes within the myeloid and lymphoid compartments circulating in individuals with trisomy 21 (T21) compared to disomic (D21) controls. A total of 36 age- and sex-matched samples were split among Palladium (Pd) barcodes, stained with antibodies, and run on a mass cytometer. Data pre-processing included normalization within and between batches via polystyrene beads embedded with lanthanides, then between batches by an empirical Bayes approach. A Barnes-Hut implementation of the t-SNE algorithm, viSNE, was utilized to visualize global structure of the immune system, then manual gating further resolved subset abundance and phenotype. Of the original sample cohort, a randomly selected subgroup of 8 whole blood samples from individuals with T21 and 8 age- and sex-matched D21 controls were stimulated directly *ex vivo* with IFNα to assay immune cell function, as determined by intensity of phospho-epitope staining among immune subtypes. **(B)** To determine appropriate viSNE parameters, all samples were subsampled, concatenated, then run through various viSNEs while altering perplexity, theta, and number of iterations. Parameters were considered optimal (Perplexity 30, bold) when biologically similar events, as denoted by color, were relatively close in proximity as well as located in diffuse rather than punctate linear formations. Examples of such fluctuations in event location while only perplexity was changed is delineated by an arrow and number while theta was set at 0.2 and the number of iterations at 10,000. Color of viSNE plots by the indicated immune subsets were determined by manual gating on canonical markers. **(C-D)** Concatenated events from individuals with T21 (n=18) and D21 controls (n=18) were **(C)** colored according to metal intensity of the indicated marker and conjugated metal isotope used to assign subsets among viSNE plots by manual gating. **(D)** Overlay of immune cell subsets (colored dots) and PhenoGraph Clusters 8 and 25 (contour plots), defined by surface marker expression on events represented in viSNE plots.

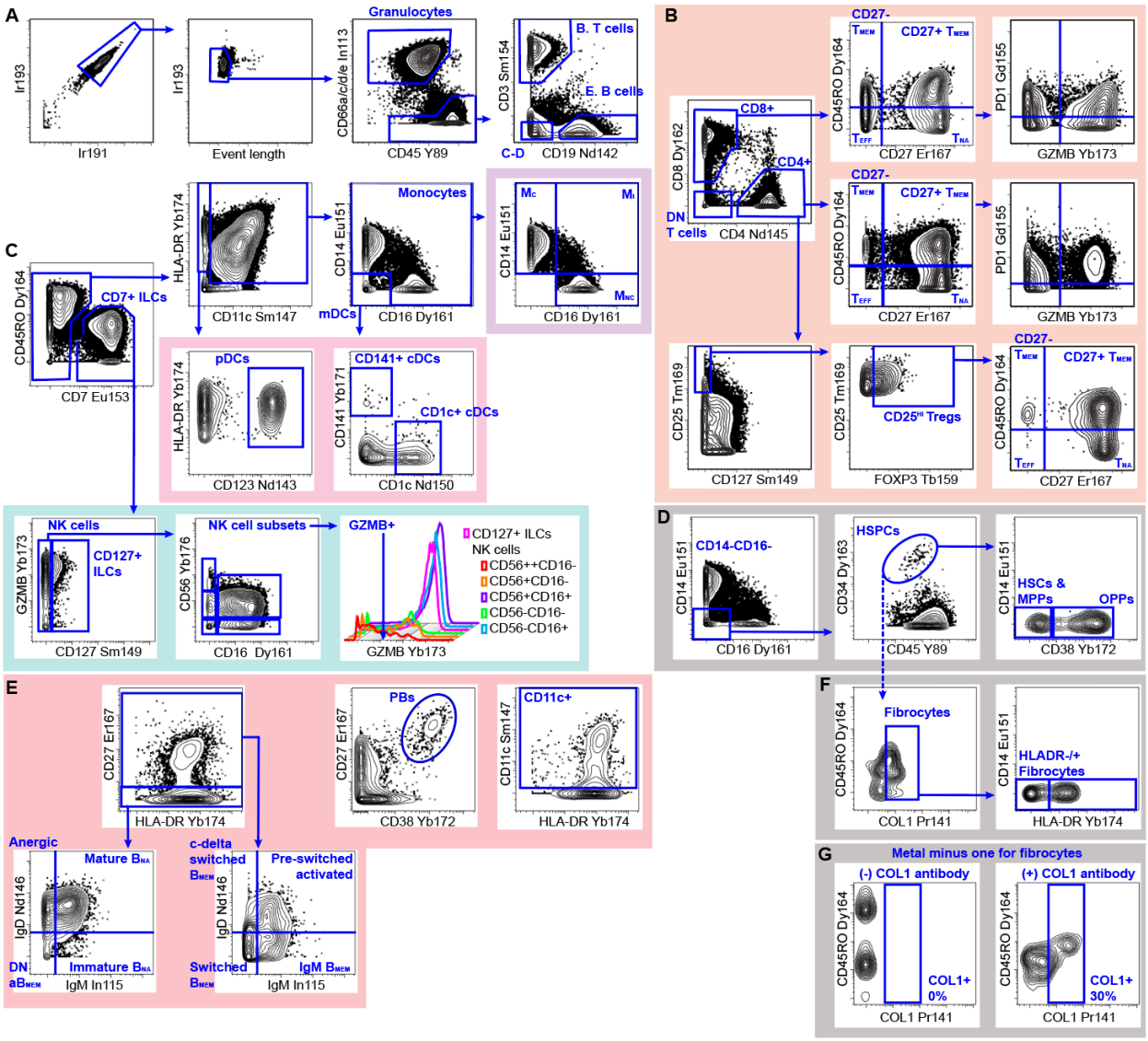

Figure S2, related to Figures 2-5. Gating scheme to resolve 100 immune cell types within the peripheral blood by mass cytometry. (A-F) Representative dot plots and histograms of mass cytometry data labeled by antibody target and isotope conjugate. **(A)** Intercalator and event length were used to identify intact single cells. Among these events, negative selection of CD66a/c/d/e was used to enrich for non-granulocytes while CD45 was used to positively identify cells of hematopoietic lineage. T and B cell lineages were identified by CD3 and CD19, respectively. **(B)** T cells were divided by CD4 and CD8 then discriminated into naïve (T_{NA}), CD27+/- memory (T_{MEM}), and effector (T_{EFF}) subsets. Among CD4+ T cells, CD25, CD127, and

FOXP3 were used to delineate $CD25^{HI}$ regulatory T cells (Tregs), which were further discriminated as described above into T_{NA}, CD27+/- T_{MEM}, and T_{EFF}. With the exception of Tregs, all CD4+ and CD8+ T cell subsets were further characterized by expression of PD1 and GZMB. T cells that did not express CD4 or CD8 were deemed double-negative (DN). **(C-D)** Among non-T or non-B cells, **(C)** monocytes were defined as CD7-, HLA-DR+, CD11c+, as well as CD14+ or CD16+, which were further used to identify classical (M_C), intermediate (M_I), and nonclassical (M_{NC}) monocyte subsets. Dendritic cells (DC) were defined through the following gating strategies: plasmacytoid DCs (pDCs) were CD7- HLADR+ CD11c- CD123+, while myeloid DCs (mDCs) were CD7- HLA-DR+ CD11c+ CD14- CD16-, and then further discriminated into CD141+ conventional DCs (cDCs) and CD1c+ cDCs. Lastly, positive expression of CD7 was interpreted as CD7+ innate lymphoid cells (ILCs) among non-T or non-B cells, from which Natural Killer (NK) cells were delineated by lack of CD127. NK cells were further divided into 5 distinct subsets by CD56 and CD16 staining. All CD7+ ILC subsets were analyzed for expression of GZMB; positive expression of this effector protein is denoted on the overlaid histograms by the position of a blue arrow. **(D)** Hematopoietic stem and progenitor cells (HSPCs) were defined among CD14- CD16- non-T or non-B cells by CD34 and CD45 staining. CD38 delineated hematopoietic stem cells (HSCs) and multipotent progenitors (MPPs) from oligopotent progenitors (OPPs). **(E)** B cells were dissected by CD27, IgD, and IgM into anergic, c-delta class switched, pre-switched, mature, and immature naïve (B_{NA}), as well as memory (B_{MEM}), which were further discriminated into IgM and IgD double-negative (DN)/atypical B_{MEM}, IgM B_{MEM}, and switched B_{MEM}. Plasmablasts (PBs) were identified by high expression of CD27 and CD38, while CD11c+ B cells were simply identified by CD11c. **(F-G)** Fibrocytes were identified in a separate experiment; gating began similar to parts “A” and “D,” as represented by a dashed line for pre-gating, to identify HSPCs among CD66-CD45+CD3-CD19-CD14-CD16- events. **(F)** COL1 was then used to identify fibrocytes followed by HLA-DR to delineate alternative phenotypes. **(G)** Positive expression for COL1 was determined by Metal Minus One

(MMO). **(A-G)** Background colors denote flow plots from distinct branches of the immune system, as described in **Table S5**.

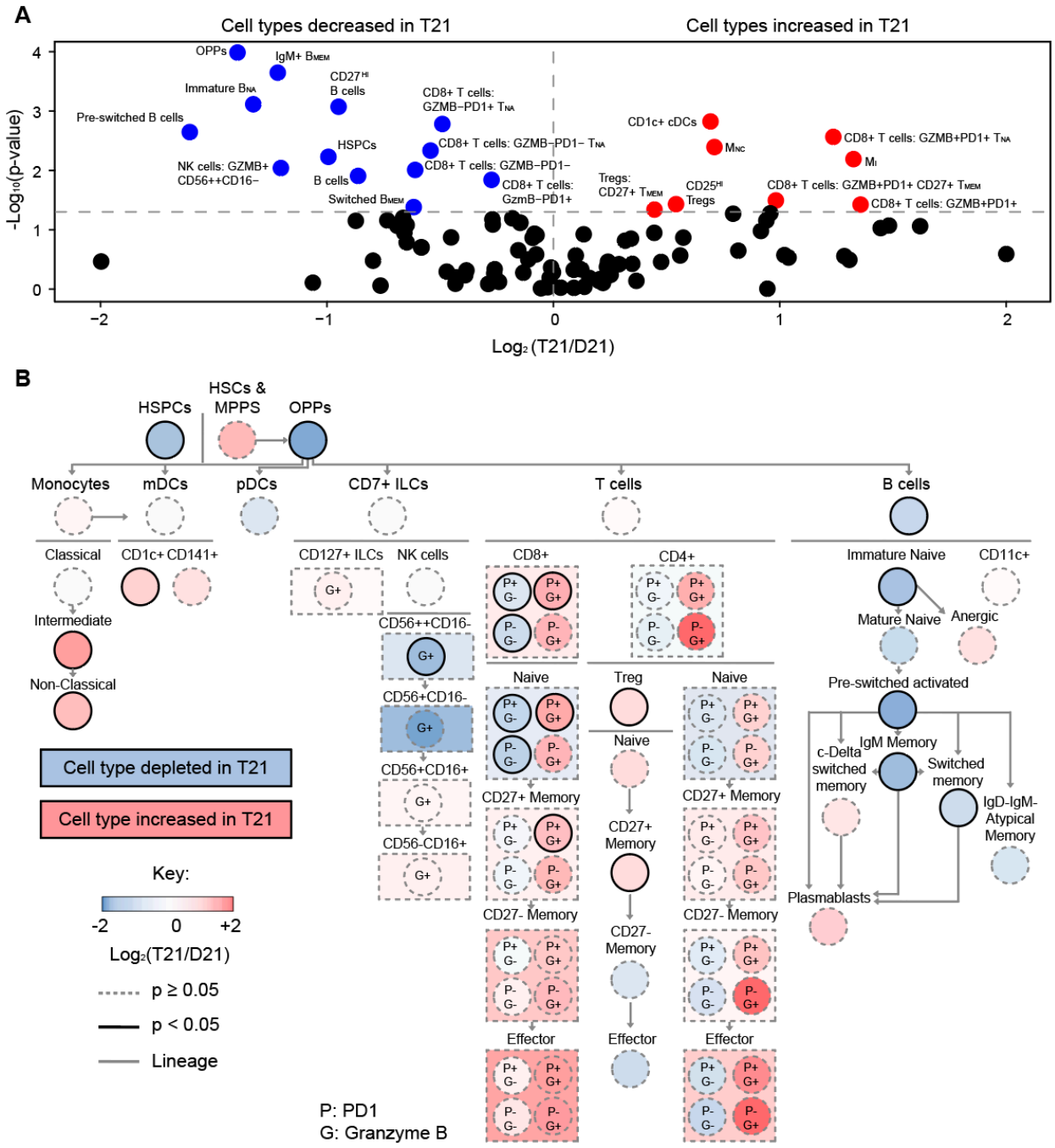

Figure S3, related to Figures 2-5. Trisomy 21 impacts every detected branch of the immune system. The frequency of 100 immune cell types simultaneously detected among non-granulocytes (CD45+CD66-) was determined by manual gating, as depicted in **Figure S2**, then compared between individuals with trisomy 21 (T21, n=18) and disomic (D21, n=18) controls. **(A)** Volcano plot displaying fold change versus p values for all 100 cell types. Dashed vertical

line represents no change, dashed horizontal line represents p≤0.05 by Student's *t* test. See **Table S4B** for full statistics. **(B)** Lineage tree depicts various immune cell types compared between individuals with T21 and D21 controls. HSPCs: hematopoietic stem and progenitor cells; HSCs: hematopoietic stem cells; MPPs: multipotent progenitor cells; OPPs: oligopotent progenitor cells, mDCs: myeloid dendritic cells, pDCs: plasmacytoid DCs, ILCs: innate lymphoid cells, NK cells: natural killer cells, Tregs: regulatory T cells. P stands for PD1 and G for Granzyme B. Color denotes fold-change where red is increased and blue is decreased frequency of immune subsets among CD45+CD66- events from individuals with T21 compared to D21 controls. In all cases, statistical difference was determined by a Student's *t* test (*p≤0.05 and **p≤0.01).

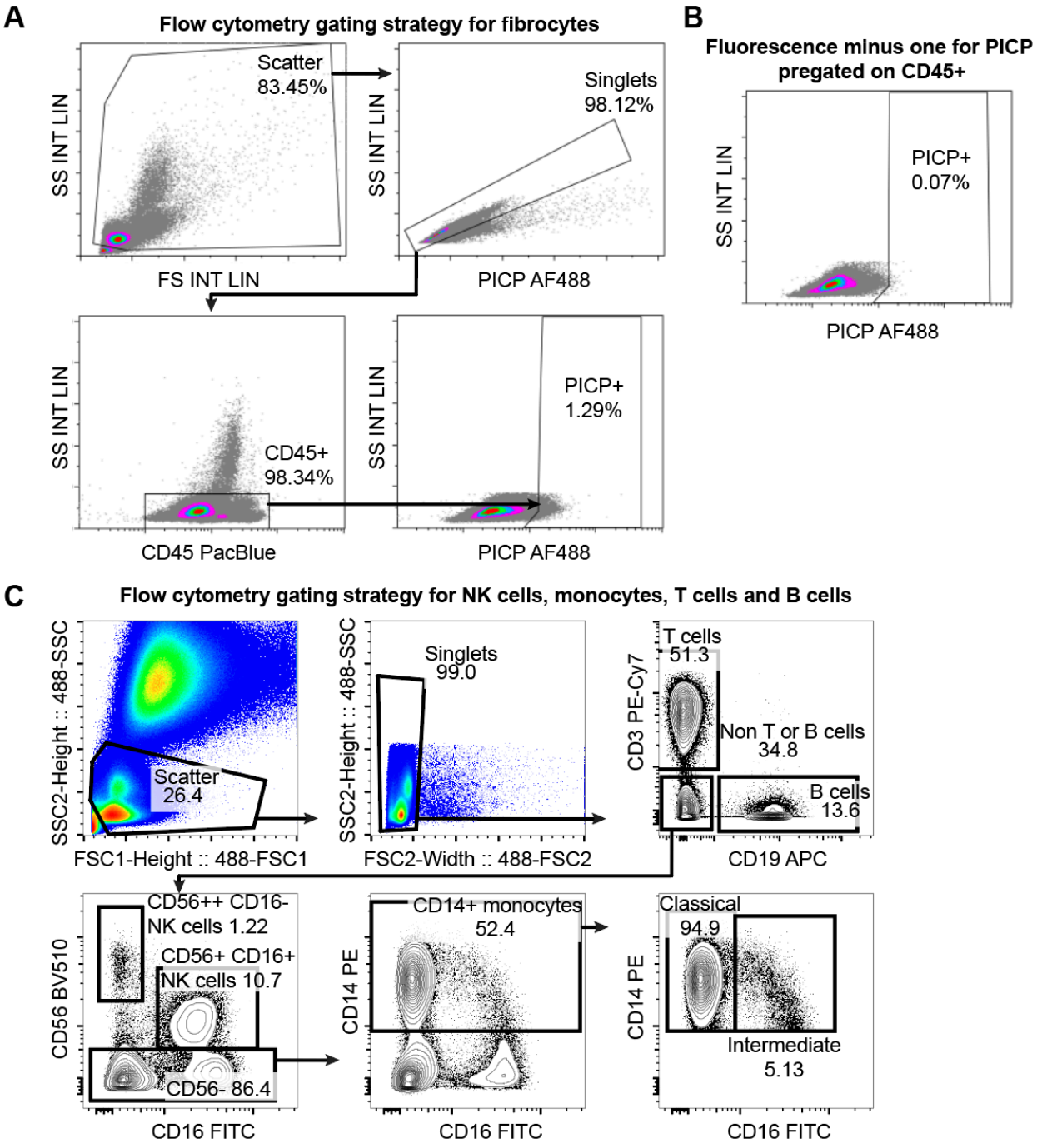

Figure S4, related to Figures 2-5. Gating scheme to identify immune subsets in the peripheral blood via flow cytometry. (A-C) Representative dot plots and histograms of flow cytometry data labeled by antibody target and isotope conjugate. **(A)** Fibrocytes were identified by positive expression of CD45 and pro-collagen I c-terminal peptide (PICP). **(B)** Positive expression of PICP was determined by fluorescence minus one (FMO). **(C)** Serial gating on

canonical markers was used to identify T cells, B cells, classical and intermediate monocytes, as well as CD56++CD6- and CD56+CD16+ NK cells.

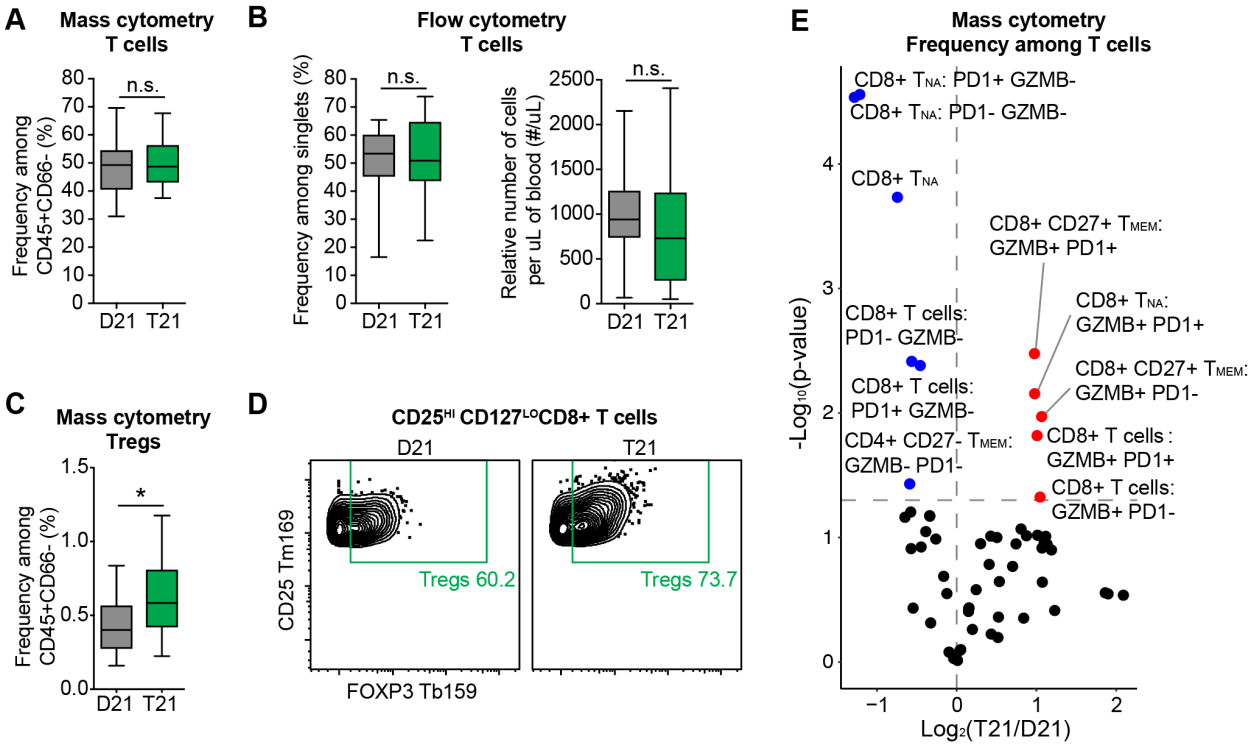

Figure S5, related to Figure 4. Analysis of the peripheral T cell compartment in people with trisomy 21. (A-B) CD3 staining was used by cytometry to quantify abundance of bulk T cells and **(C-E)** T cell subsets within the peripheral blood of individuals with trisomy 21 (T21) and disomic (D21) controls, as described in **Figure S2A-B, Figure S4C,** and **Table S5**. **(A)** Mass cytometry was used to determine the frequency of bulk T cells among non-granulocytes of hematopoietic lineage (CD45+CD66-) within the peripheral blood of individuals with T21 (n=18) and D21 controls (n=18), as described in **Figure S2A-B**. **(B)** Flow cytometry and complete blood counts were used to determine the frequency and relative number of bulk T cells among single events within the peripheral blood of individuals with T21 (n=39) and D21 controls (n=50), as described in **Figure S4C**. **(C-D)** Within mass cytometry data, FOXP3 expression was used to determine the frequency of regulatory T cells (Tregs) among non-granulocytes of hematopoietic lineage (CD45+CD66-) within the peripheral blood of individuals with T21 (n=18) and D21 controls (n=18), as described in **Figure S2A-B**. **(D)** Representative examples of Treg frequency among the parent gate of $CD25^{HI}$ $CD127^{LO}$ CD8+ T cells. **(E)** The frequency of all detected T

cell subsets was simultaneously detected among bulk T cells by manual gating, as depicted in **Figure S2A-B and Table S5**, then compared between individuals with T21 (n=18) and D21 (n=18) controls. Volcano plot depicts fold change versus p values for all 57 subsets of T cells. Dashed vertical line represents no change, dashed horizontal line represents $p \leq 0.05$ by Student's *t* test. See **Table S4C** for full statistics and acronym meaning. **(A-E)** All statistical significance was determined by a Student's *t* test, *$p \leq 0.05$, **$p \leq 0.01$, ***$p \leq 0.001$, and ****$p \leq 0.0001$.

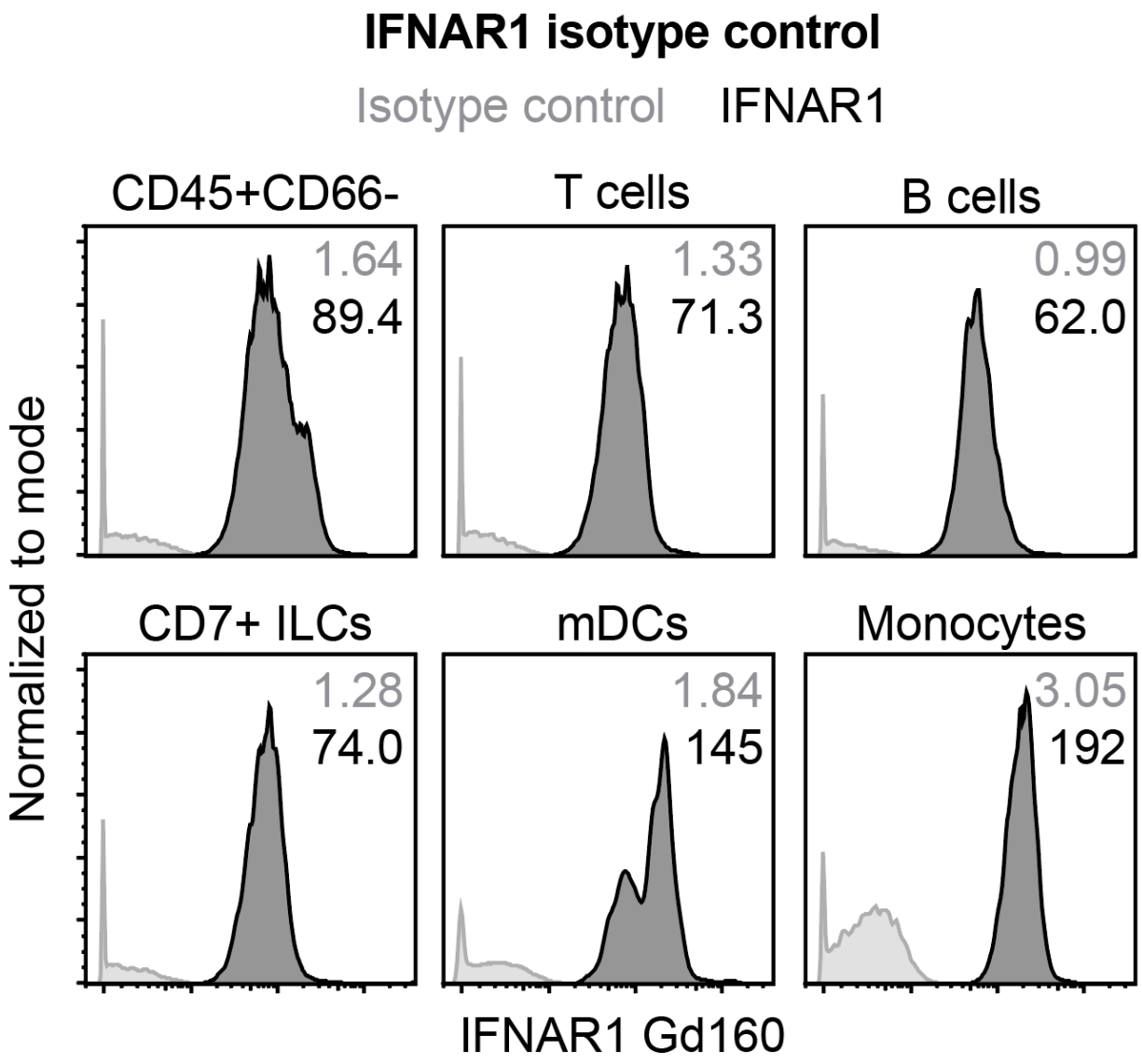

Figure S6, related to Figure 6. IFNAR1 isotype control. As done for the antibody against IFNAR1 described in **Table S3**, a recombinant Rabbit IgG isotype control (Abcam ab199376) was conjugated to the metal isotype Gd160 using the Maxpar Antibody Labeling Kit (Fluidigm 201160B), tittered, and used to stain a representative D21 control sample side-by-side with the anti-IFNAR1-Gd160. Staining by isotype control is indicated in grey histograms and grey geometric mean metal intensities (gMMIs) while staining by anti-IFNAR1 is similarly denoted in black.

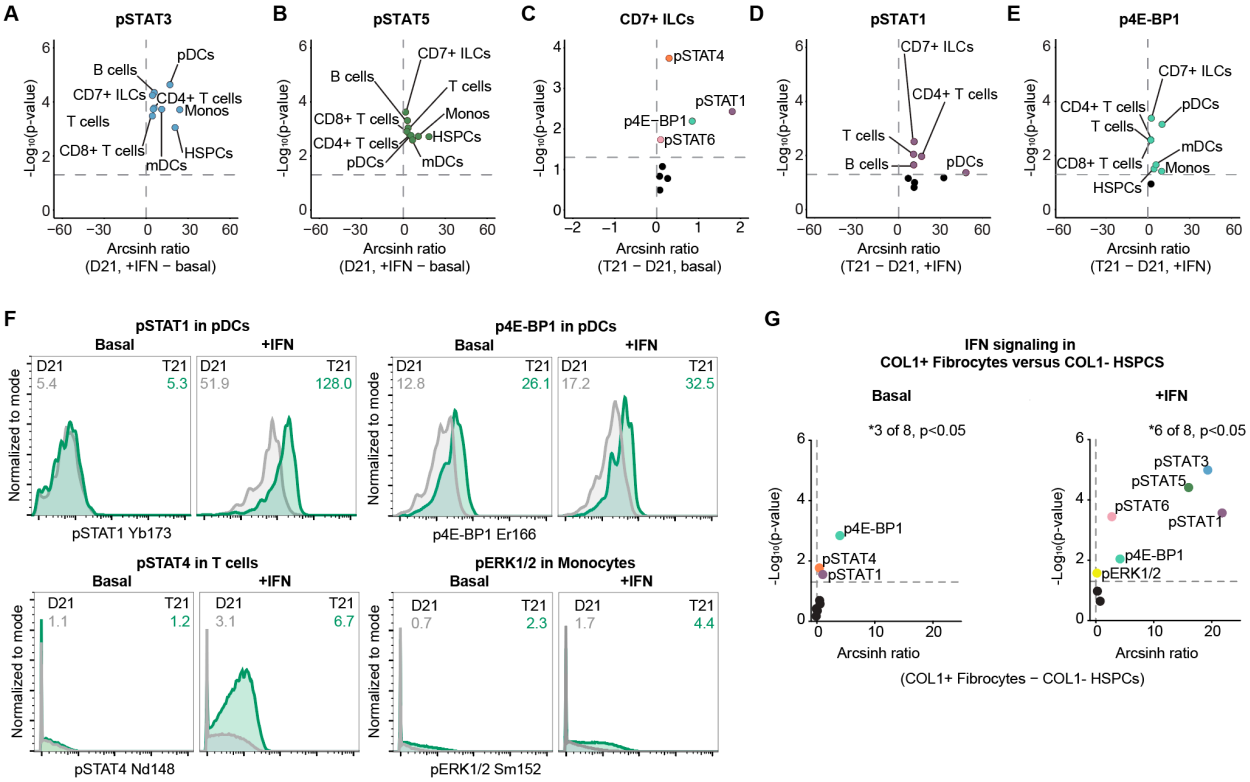

Figure S7, related to Figure 7. Immune cells with trisomy 21 are hyperresponsive to IFNα.

(A-G) Whole blood was incubated directly *ex vivo* for 30 mins with (+IFN) or without (basal) IFNα-2a (10,000 U/mL), then processed for mass cytometry according to **Figure S1**. Phospho-epitopes among bulk immune subtypes were resolved by manual gating on expression of canonical markers as depicted in **Figure S2** among individuals with trisomy 21 (T21, n=8) and disomic (D21, n=8) controls. Induction of **(A)** pSTAT3 and **(B)** pSTAT5 in 9 diverse immune subsets within the D21 cohort following IFNα stimulation. **(C)** Basal levels of phospho-epitopes in CD7+ innate lymphoid cells (ILCs) from individuals with T21 compared to D21 controls. **(D-E)** Immune subsets with significant **(D)** pSTAT1 and **(E)** p4E-BP1 levels following IFNα stimulation from individuals with T21 compared to D21 controls. **(F)** Representative histograms and gMMIs of phospho-epitopes among indicated immune subsets from an individual with T21 (green) and a D21 control (grey). **(G)** Levels of phospho-epitopes in COL1+ Fibrocytes compared to COL1- Hematopoietic stem and progenitor cells (HSPCs) from individuals with T21 and D21 controls

(n=16 per COL1 group) both without (left volcano plot) and with (right volcano plot) IFNα stimulation. COL1 gating was done according to **Figure S2. (A-E, and G)** Arcsinh ratios and p-values were calculated from geometric mean metal intensities (gMMIs). All statistical significance was determined by a Student's *t* test and the horizontal dashed line represents statistical significance where $p \leq 0.05$; please see **Table S4C** for full statistics.